Journal of Quality Measurement and Analysis
e-ISSN: 2600-8602
https://doi.org/10.17576/jqma.2104.2025.07

JQMA 21(4) 2025, 117-134
http://www.ukm.my/jqma

EXPLORING NOVEL INSIGHTS ON MHD MIXED CONVECTION WITH TRI-HYBRID NANOFLUID ON AN INCLINED SHEET WITH SUCTION EFFECTS

ARFAN HYDER, YEON JIANN LIM*, ILYAS KHAN & SHARIDAN SHAFIE

ABSTRACT

The study of ternary hybrid nanofluid (THNF) over inclined stretching/shrinking surfaces under the influence of various physical effects is crucial for optimizing heat transfer processes in engineering applications. This numerical investigation aims to provide novel insights by comprehensively analyzing the mixed convective flow and heat transfer characteristics of THNF comprising Cu, TiO_2, and Al_2O_3 nanoparticles dispersed in water. The study uniquely considers the combined effects of thermal radiation, magnetohydrodynamics, and suction/injection on the THNF flow over an inclined stretching/shrinking sheet. The Keller box method is employed to numerically solve ordinary differential equations derived from governing nonlinear partial differential equations using similarity transformation. The influence of pertinent parameters, including suction/injection, mixed convection, stretching/shrinking, magnetic field, and radiation, on the profiles of temperature and velocity, as well as the rate of heat transfer, is elucidated through graphical and tabular representations validated against previous literature. Findings reveal that increasing the suction parameter enhances heat transfer rate by 6.65%, while increasing the inclination angle reduces it by 0.21%. This study contributes to the growing knowledge on THNF by providing valuable insights into their flow behavior and heat transfer characteristics, with potential applications in engineering and industrial domains such as enhanced heat exchangers, solar energy systems, and advanced thermal control technologies.

Keywords: ternary hybrid nanofluid; suction/injection; Keller-box method; inclined plate; stretching/shrinking

1. Introduction

Ternary hybrid nanofluids (THNFs) represent an emerging frontier in the field of fluid dynamics, with considerable promise for improving heat transfer performance and fluid flow behavior compared to conventional working fluids. These advanced nanofluids contain three distinct nanoparticles suspended within a base fluid, forming a composite that outperforms mononanofluids and binary hybrids in terms of thermal conductivity and energy transport efficiency (Hanif *et al.* 2023; Alqarni *et al.* 2023). Recent research has focused on combining nanoparticles like copper (Cu), aluminum oxide (Al_2O_3), and titanium dioxide (TiO_2) with water to develop THNF that exhibit superior thermophysical properties. This multi-component suspension benefits from the synergistic interactions between the nanoparticles and the base fluid, increasing heat transfer rates and thermal stability (Nath & Deka 2024; Ouyang *et al.* 2024c). The collective behavior of the nanoparticles contributes to an efficient mechanism for improving thermal performance in diverse engineering systems. A study by Usman *et al.* (2023) explored the heat transfer properties of a THNF comprising Cu, TiO_2, and Al_2O_3 dispersed in water under inclined flow conditions. Their findings revealed a noticeable improvement in thermal performance, attributed to the enhanced surface area and thermal conductivity offered by the nanoscale particles. Such nanofluids demonstrate improved heat dissipation over traditional fluids due to their high surface area-to-volume ratios.

The potential applications of THNF span numerous industrial domains. For instance, Sarfaz and Khan (2023) evaluated the behavior of THNF in Hiemenz and Homann flow regimes,

reporting significant gains in thermal conductivity, energy transport, and wall shear stress compared to conventional fluids. These enhancements underscore the value of THNF in sectors such as energy systems, electronic cooling, biomedical devices, and environmental technologies. Further, Ouyang *et al.* (2024b) studied the behavior of THNF in porous media influenced by heat generation and absorption effects. Their results indicated an approximate 20.38% improvement in thermal performance relative to mono-nanofluids, reinforcing the viability of THNF as efficient agents for heat transfer enhancement in complex environments. Dispersions of nanoparticles in the THNF significantly increased polymer thermophysical properties as well, which points to thermal management system applications. The various improvements demonstrated by THNF necessitate more studies along these directions.

Algehyne *et al.* (2022) studied energy and mass transportation in THNF flow across a stretched permeable surface. Their study determined that fluid energy and velocity propagation rates were enhanced when ternary hybrid nanocomposites were added compared to simple nanofluids. Noteworthy is that the base fluid exhibited a thermal conductivity increased by as much as 61% by adding ternary hybrid nanoparticles. These exceptional enhancements of thermophysical properties are a testament to THNF's promise as a means to enable more efficient heat exchangers, cooling systems, and various thermal management applications. The findings have practical applications to inform further improvements of superior thermal management systems in a vast array of industrial and technological applications. Noreen *et al.* (2023) analyzed a THNF's thermofluid characteristics when it is passing through parallel discs and incorporates MHD effects. By employing the Cattaneo-Christov heat flux model, it was determined via numerical simulations that velocity, temperature, as well as nanoparticle concentration profiles, were considerably influenced. The results indicated increased thermal conduction when a larger fraction of nanoparticles is employed in a given THNF. These results have technological significance in engineering and medicine and biomedical applications. Some recent investigations have explored THNF's remarkable properties and performances, and emphasized its potential to revolutionize heat transfer processes and fluid flow applications.

Mixed convection, through the combined action of both natural and forced convection, is responsible for a remarkable share in thermal behavior of nanofluids in a vast majority of applications (Lund *et al.* 2022; Hyder *et al.* 2023). The role of the mixed convection parameter in ptimising flow behaviour as well as heat transfer effectiveness has been addressed by Kadhim Hussein *et al.* (2024) and Ali *et al.* (2024b) in scenarios when external flow forces are combined with buoyancy effects. Incorporating mixed convection considerations into THNF studies enables a more comprehensive understanding of how buoyancy-driven and externally imposed flows influence temperature fields and velocity distributions. This coupling between thermal gradients and flow velocities is especially relevant for systems requiring precise thermal control. By examining the effects of mixed convection on ternary hybrid nanofluids, researchers can better tune parameters such as thermal conductivity, flow structure, and energy transport to suit specific engineering needs. Such insights are crucial for improving heat exchanger performance, electronic cooling, and microscale fluidic applications. Vanitha *et al.* (2022) studied mixed convection flow of a viscoelastic fluid over a permeable stretching sheet, considering additional effects like suction/injection, thermophoresis, and radiation. The study found that nanoparticle transportation is significantly affected by the Richardson number, resulting in a few solution branches when Prandtl numbers are greater. The model, however, ignored thermal radiation effects that could be applied to forecast accuracy when heat transfer is radiative. Das *et al.* (2022) presented a theoretical framework to study mixed convection flow of ionized THNFs through a vertical channel, accounting for magnetic field and electric double layer (EDL) effects. The results revealed that both magnetic strength and Debye-Hückel length significantly alter flow characteristics, and hence have potential applications in nanofluidic devices, micropumps, and solar-based devices. Nevertheless, the study did not account for mass transfer mechanisms such as suction or injection, which may further influence heat and mass transport characteristics.

Farooq *et al.* (2024) conducted a study on the mixed convection flow of ternary hybrid

nanofluids (THNF) near a vertical Riga plate, formulating the model using the conservation principles of momentum and energy. To manage the complexity of the governing equations, they applied a nonsimilar variable transformation, converting the problem into nonlinear partial differential equations. The transformed system was then addressed using a local nonsimilarity solution method. Their findings revealed that an increase in the mixed convection parameter results in a significant reduction in the local skin friction coefficient. Takreem and Satya Narayana (2024) examined the thermal performance of a THNF flowing over a stretched surface when it is subject to flow conditions of mixed convection. The model entailed the incorporation of a Cattaneo–Christov heat flux model that ensures non-Fourier effects during heat conduction are incorporated. The results indicated that the THNF exhibited enhanced heat transfer efficiency as compared to both mono and binary nanofluids. The velocity of fluid increased as more substantial mixed convection parameter values were employed, but substantial radiation parameter values significantly increased the temperature distribution. The working fluid utilized was a suspension of titanium dioxide, copper, and aluminum oxide nanoparticles in water. The surface exhibited both shrinking and stretching behavior.

Adnan *et al.* (2024) examined flow of a water-based THNF around a cylindrical geometry influenced by mixed convection, resistive heating, and an externally applied magnetic field. Their analysis indicated that the ternary nanoliquid exhibited a faster temperature rise than its hybrid or conventional counterparts, primarily due to the synergistic thermal effects of the three nanoparticles. Additionally, enhanced mixed convection intensified the shear drag along a cylindrical surface. Through extensive parametric studies, the authors highlighted the role of internal heat generation and buoyancy effects in regulating temperature profiles within complex nanoliquid systems. Despite these advancements, it is important to note that the study did not consider the combined influence of thermal radiation, suction, and injection mechanisms, which constitute key limitations of their work. Mishra *et al.* (2023) evaluated the thermal transport and flow behavior of THNF considering changes in the injection and suction parameter. The study found that increased rates of injection or suction were followed by decreased velocity profiles which implied improved thermal performance due to increased fluid surface interactions. This parameter serves as a practical means for modulating temperature fields, flow structures, and convective heat transfer rates within THNF systems. The ability to adjust these dynamics offers significant potential for optimizing thermal control in engineering applications.

In addition, the analysis of thermal and fluid transport over inclined surfaces has attracted increasing interest owing to its broad applicability in engineering design. An inclined surface is defined by its deviation from the horizontal or vertical axis, characterized by a specific angle of inclination. Such configurations are frequently encountered in structural and thermal engineering, for instance, in ramps, sloped surfaces, and architectural elements where understanding inclination effects is crucial for assessing mechanical stability and heat distribution, as highlighted by Eid *et al.* (2023). The analysis of heat and fluid flow transfer over sloping geometries at various angles is essential in boosting thermal management systems' performance, e.g., in solar thermal collectors, electronic cooling systems, and compact heat exchangers. Surface inclination can significantly influence boundary layer development and thermal gradients, thus affecting system efficiency. Despite its importance, the behavior of nanofluid, particularly THNF, over inclined surfaces has not been extensively investigated, leaving room for further exploration aimed at improving energy efficiency and operational sustainability (Sohut *et al.* 2023; Anuar *et al.* 2021).

Moreover, considerable interest has been shown in flow over stretching and shrinking surfaces placed at inclined orientations. These configurations are particularly relevant in advanced manufacturing and coating processes, as noted in recent studies (Alabdulhadi *et al.* 2021; Ouyang *et al.* 2024a), making them a compelling area for ongoing research. Lund *et al.* (2020) explored fluid flow and thermal transport through a shrinking and stretching surface that was inclined. The study entailed micropolar nanofluids with convective boundary conditions and determined that stability analysis is performed and dual solutions are observed. The results established that both increased inclination angle parameter and buoyancy parameter made both

skin friction and mass transfer rate rise through both solution curves. However, the heat transfer rate possessed a different trend such that a reverse flow behavior is noted. According to it, Jeelani and Abbas (2023) also investigated a stretched inclined surface exposed to suction and magnetic influence. The paper employed Al_2O_3 and copper nanoparticles in ethylene glycol and modeled them as a non-Newtonian Maxwell fluid. The prominent finding that emerged out of it is that velocity profiles were found to increase when there is an escalation of the inclination angle parameter.

Ali *et al.* (2022) analyzed the thermal characteristics of a fluid environment subjected to periodic variations in gravity, alongside mixed convective motion and magnetic influences. Their work specifically addressed micropolar and hybrid nanofluid flows over an angled surface. It was noted that enhancing the magnetic field strength led to a rise in fluid temperature, whereas increasing the inclination angle resulted in lower values for both rate of heat transfer and skin friction. Ali *et al.* (2021b) explored how suction and injection mechanisms affect a micropolar fluid's mixed convection flow under the modulation of gravitational forces. Their investigation also considered magnetic field effects and thermal radiation near an inclined boundary layer. The study focused on determining how these variables suction, injection, magnetism, and radiative heat shape the flow structure and thermal convection behavior adjacent to the sloped wall.

This paper examines the behavior of heat and flow transfer in a THNF moving along an inclined surface subjected to both stretching and shrinking motions, inspired by its strong potential to enhance thermal efficiency. The analysis incorporates several critical physical phenomena, including the influences of mixed convection, fluid suction and injection, magnetic field interactions, thermal radiation, shrinking and the stretching parameters. The THNF utilized comprises copper, titanium dioxide (TiO_2), and aluminum oxide (Al_2O_3) nanoparticles dispersed in water as the base liquid. A thorough review of existing studies reveals that none have simultaneously considered all these parameters in the context of THNF, highlighting the originality and comprehensive nature of this research. The governing equations of momentum and energy are initially framed as partial differential equations. These are subsequently simplified through an appropriate similarity transformation, resulting in a system of nonlinear ordinary differential equations. The Keller box method, a robust and widely adopted implicit finite difference scheme, is employed to solve the reduced system. The study presents detailed graphical representations of the temperature and velocity fields, along with numerical results for the skin friction coefficient and Nusselt number, all obtained using MATLAB.

To validate the reliability and accuracy of the numerical results, comparisons are made with existing results from previous research, presented in tabulated form. This comprehensive methodology deepens insights into the complex relationships among key physical parameters and their effects on the thermofluid behavior of THNF within the studied flow context. This research addresses a notable gap in the current literature by examining the collective influence of multiple governing parameters on the thermal and flow behavior of THNF. By providing a more integrated perspective, this study provides new insights into how parameters such as suction and injection, inclination angle, and magnetic field (MHD) interactions can be strategically used to enhance heat transfer in applied engineering systems. The outcomes not only strengthen the theoretical framework surrounding THNF flows but also contribute to the design of practical technologies, including efficient heat exchangers, solar thermal devices, and advanced cooling systems.

In pursuit of these objectives, the study aims to respond to the following research questions:

- How does the inclination angle influence the flow characteristics and heat transfer rate?
- What is the combined effect of MHD, suction/injection, mixed convection, thermal radiation and stretching/shrinking parameters on the performance of THNF?

2. The Governing Equations

The study investigates the steady, two-dimensional, incompressible, and laminar flow of a ternary hybrid nanofluid (THNF) over an inclined plate undergoing stretching or shrinking. The flow is affected by mixed convection and subjected to a uniform magnetic field oriented perpendicular to the plate surface. The velocity of the stretching or shrinking surface is assumed to vary linearly along the horizontal coordinate, described by $u = u_w = ax$, where $a > 0$ is a constant representing the stretching rate. The surface temperature of the plate, denoted by T_w, also varies linearly with the streamwise coordinate and is expressed as $T_w = T_\infty + bx$. In this expression, b represents a constant temperature gradient or rate of temperature change along the plate, and T_∞ is the ambient or free-stream temperature of the nanofluid. This constant temperature gradient b has physical significance, quantifying the rate of temperature change per unit length along the plate. A higher b indicates a faster temperature rise, while a lower b suggests a slower temperature rise (Dawar *et al.* 2022). The conceptual framework is illustrated in Figure 1. Subject to the stated assumptions, the corresponding governing equations are formulated as follows (Anuar *et al.* 2021):

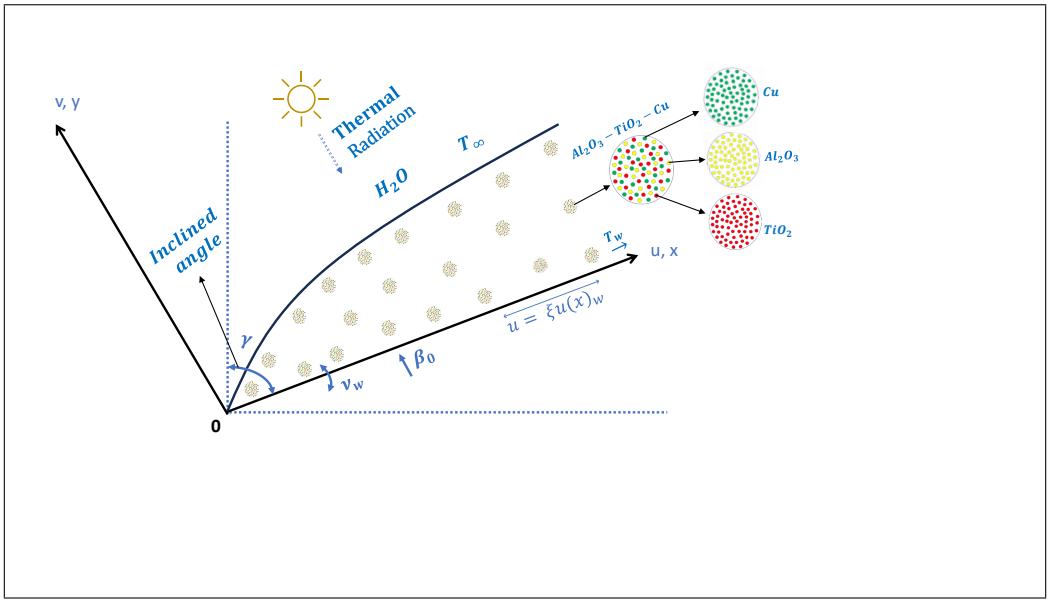

Figure 1: Schematic diagram of the physical flow configuration

$$\frac{\partial u}{\partial x} + \frac{\partial v}{\partial y} = 0 \tag{1}$$

$$u\frac{\partial u}{\partial x} + v\frac{\partial u}{\partial y} = \nu_{thnf}\frac{\partial^2 u}{\partial y^2} + \frac{(\rho\beta)_{thnf}}{(\rho)_{thnf}}(T - T_\infty)g\cos\gamma - \frac{\sigma_{thnf}}{\rho_{thnf}}B_0^2(u) \tag{2}$$

$$u\frac{\partial T}{\partial x} + v\frac{\partial T}{\partial y} = \frac{k_{thnf}}{\rho_{thnf}(C_P)_{thnf}}\left(\frac{\partial^2 T}{\partial y^2}\right) - \frac{1}{(\rho C_P)_{thnf}}\frac{\partial q_r}{\partial y} \tag{3}$$

The vertical and horizontal velocity components are denoted by v and u, respectively. The kinematic viscosity of the ternary hybrid nanofluid (THNF) is represented by ν_{thnf}, defined as $\nu_{thnf} = \mu_{thnf}/\rho_{thnf}$, where μ_{thnf} and ρ_{thnf} are the dynamic viscosity and density of the THNF, respectively. The electrical conductivity of the THNF is expressed as σ_{thnf}, while the externally applied magnetic field strength is given by B_0^2. The fluid temperature is represented

by T, and the gravitational acceleration is indicated by g. The radiative heat flux is indicated by q_r, and the thermophysical parameters of the THNF, namely, the specific heat capacity, thermal conductivity, and coefficient of thermal expansion are given by $(\rho C_p)_{thnf}$, k_{thnf}, and β_{thnf}, respectively. A comprehensive formulation of the thermophysical properties corresponding to the nanoparticles used in the THNF is summarized in Table 1.

Table 1: Mathematical expression for thermophysical properties of nanofluid, HNF and THNF (Chen *et al.* 2023; Ramzan *et al.* 2023)

Dynamic Viscosity:

$$\mu_{thnf} = \frac{\mu_f}{(1-\phi_1)^{2.5}(1-\phi_2)^{2.5}(1-\phi_3)^{2.5}}.$$
$$\mu_{hnf} = \frac{\mu_f}{(1-\phi_1)^{2.5}(1-\phi_2)^{2.5}}.$$
$$\mu_{nf} = \frac{\mu_f}{(1-\phi_1)^{2.5}}.$$

Density

$$\rho_{thnf} = (1-\phi_1-\phi_2-\phi_3)\rho_f + \phi_1\rho_1 + \phi_2\rho_2 + \phi_3\rho_3.$$
$$\rho_{hnf} = (1-\phi_1-\phi_2)\rho_f + \phi_1\rho_1 + \phi_2\rho_2.$$
$$\rho_{nf} = (1-\phi_1)\rho_f + \rho_1\phi_1.$$

Heat Capacity:

$$(\rho C_P)_{thnf} = (1-\phi_1-\phi_2-\phi_3)(\rho C_P)_f + \phi_1(\rho C_P)_1 + \phi_2(\rho C_P)_2 + \phi_3(\rho C_P)_3.$$
$$(\rho C_P)_{hnf} = (1-\phi_1-\phi_2)(\rho C_P)_f + \phi_1(\rho C_P)_1 + \phi_2(\rho C_P)_2.$$
$$(\rho C_P)_{nf} = (1-\phi_1)(\rho C_P)_f + \phi_1(\rho C_P)_1.$$

Thermal Expansion:

$$(\rho\beta)_{thnf} = (1-\phi_1-\phi_2-\phi_3)(\rho\beta)_f + \phi_1(\rho\beta)_1 + \phi_2(\rho\beta)_2 + \phi_3(\rho\beta)_3.$$
$$(\rho\beta)_{hnf} = (1-\phi_1-\phi_2)(\rho\beta)_f + \phi_1(\rho\beta)_1 + \phi_2(\rho\beta)_2.$$
$$(\rho\beta)_{nf} = (1-\phi_1)(\rho\beta)_f + \phi_1(\rho\beta)_1.$$

Thermal Conductivity:

$$\frac{k_{thnf}}{k_{hnf}} = \frac{k_3 + 2k_{hnf} + 2\phi_3(k_3 - k_{hnf})}{k_3 + 2k_{hnf} - \phi_3(k_3 - k_{hnf})}.$$
$$\frac{k_{hnf}}{k_{nf}} = \frac{k_2 + 2k_{nf} + 2\phi_2(k_2 - k_{nf})}{k_2 + 2k_{nf} - \phi_2(k_2 - k_{nf})}.$$
$$\frac{k_{nf}}{k_f} = \frac{k_1 + 2k_f + 2\phi_1(k_1 - k_f)}{k_1 + 2k_f - \phi_1(k_1 - k_f)}.$$

Electrical Conductivity:

$$\frac{\sigma_{thnf}}{\sigma_{hnf}} = \frac{\sigma_3(1+2\phi_3) + \sigma_{hnf}(1-2\phi_3)}{\sigma_3(1-\phi_3) + \sigma_{hnf}(1+\phi_3)}.$$
$$\frac{\sigma_{hnf}}{\sigma_{nf}} = \frac{\sigma_2(1+2\phi_2) + \sigma_{nf}(1-2\phi_2)}{\sigma_2(1-\phi_2) + \sigma_{nf}(1+\phi_2)}.$$
$$\frac{\sigma_{nf}}{\sigma_f} = \frac{\sigma_1(1+2\phi_1) + \sigma_f(1-2\phi_1)}{\sigma_1(1-\phi_1) + \sigma_f(1+\phi_1)}.$$

The corresponding boundary conditions applied in this study are outlined below, as referenced in (Yasir *et al.* 2023):

$$\begin{aligned} y = 0: &\quad u = u_w(x)\xi, \quad v = v_w, \quad T = T_w(x), \\ y \to \infty: &\quad u \to 0, \quad T = T_\infty. \end{aligned} \tag{4}$$

In this context, the constant mass flux velocity is denoted by v_w, where a negative value ($v_w < 0$) corresponds to the case of suction, while a positive value ($v_w > 0$) indicates injection.

Additionally, the parameter ξ characterizes the shrinking or stretching behavior of the sheet; specifically, $\xi < 0$ signifies a shrinking sheet, whereas $\xi > 0$ refers to a stretching sheet. In the present study, the THNF is assumed to be optically thick. As a result, the Rosseland approximation is employed to account for the effects of thermal radiation within the boundary layer analysis. The radiative heat transfer is modeled through the Stefan–Boltzmann constant, denoted by σ^*, and the Rosseland mean absorption coefficient, represented by k^*.

$$q_r = -\frac{4}{3}\frac{\sigma^*}{k^*}\frac{\partial T^4}{\partial y} \tag{5}$$

The Taylor series expansion for T^4 around the constant temperature T_∞ is performed. In this process, higher-order terms are disregarded, yielding the result:

$$T^4 \approx 4T_\infty^3 T - 3T_\infty^4. \tag{6}$$

When incorporating Eqs. (5) and (6) into the Eq. (3), the result is

$$u\frac{\partial T}{\partial x} + v\frac{\partial T}{\partial y} = \frac{k_{nf}}{(\rho C_P)_{nf}}\left(\frac{\partial^2 T}{\partial y^2}\right) + \frac{1}{(\rho C_P)_{nf}}\frac{16}{3}\frac{\sigma^*}{k^*}T_\infty^3\left(\frac{\partial^2 T}{\partial y^2}\right) \tag{7}$$

3. Similarity Transformation

Suitable similarity variables are introduced, which transform the original governing equations into a corresponding system of ordinary differential equations (ODEs). The process of non-dimensionalization and transformation of Eqs. (1), (2) and (7) is facilitated by utilizing the subsequent similarity variables (Wahid *et al.* 2023):

$$\psi(x,y) = (a\nu_f)^{1/2} x f(\eta), \quad \theta(\eta) = \frac{T - T_\infty}{T_w - T_\infty}, \quad \eta = y\left(\frac{a}{\nu_f}\right)^{1/2}. \tag{8}$$

The stream function $\psi = \psi(x,y)$ is typically formulated in the form of $u = \frac{\partial \psi}{\partial y}$ and $v = -\frac{\partial \psi}{\partial x}$, in accordance with the continuity Eq. (1). Upon substitution these transformations into the momentum Eq. (2) and energy Eq. (7), we obtain the subsequent outcomes:

$$\left[\frac{\mu_{thnf}}{\mu_f}\right] f''' + \left[\frac{\rho_{thnf}}{\rho_f}\right]\left(ff'' - f'^2\right) + \left[\frac{(\rho\beta)_{thnf}}{(\rho\beta)_f}\right]\lambda\theta\cos\gamma - \left[\frac{\sigma_{thnf}}{\sigma_f}\right] M_g f' = 0 \tag{9}$$

$$\left[\frac{k_{thnf}}{k_f}\right](1+R_d)\theta'' + \left[\frac{(\rho C_P)_{thnf}}{(\rho C_p)_f}\right] Pr\left(f\theta' - f'\theta\right) = 0 \tag{10}$$

In these equations, the prime notation signifies differentiating with respect to η. Table 2 presents the dimensionless key parameters employed in the present study.

The boundary conditions (4) transform into nondimensional as:

$$\left.\begin{array}{llll} f'(0) = \xi, & f(0) = s \quad \theta(0) = 1, & \text{at} & \eta = 0. \\ f'(\eta) = 0, & \theta(\eta) = 0, & \text{at} & \eta \to \infty. \end{array}\right\} \tag{11}$$

Table 3 provides a compilation of the thermophysical parameters for the THNF under investigation, based on the referenced sources. The symbol ϕ denotes the volume fractions of the

Table 2: Key parameters and their formulas

Parameter	Formula
Magnetic interaction parameter.	$M_g = \dfrac{\sigma_f B_0^2}{a\rho_f}$
Radiation parameter.	$R_d = \dfrac{16}{3}\dfrac{\sigma^*}{k^*}\dfrac{T_\infty^3}{k_{hnf}}$
Prandtl number.	$Pr = \dfrac{\nu_f}{\alpha_f} = \dfrac{(\mu C_p)_f}{k_f}$
Mixed convection parameter.	$\lambda = \dfrac{Gr_x}{(Re_x)^2}$
Local Grashof number.	$Gr_x = \dfrac{g\beta_f(T_w - T_\infty)x^3}{\nu_f^2}$
Local Reynolds number.	$Re_x = \dfrac{u_w x}{\nu_f}$
Suction/injection parameter.	$s = \dfrac{-v_w}{(a\nu_f)^{1/2}}$

nanoparticles, with a consistent subscript notation throughout: $()_1$, $()_2$, and $()_3$ represent the thermophysical characteristics of titanium, aluminum, and copper nanoparticles, respectively. The subscripts $()_f$, $()_{nf}$, $()_{hnf}$, and $()_{thnf}$ refer to the base fluid, nanofluid, hybrid nanofluid, and THNF, respectively.

Table 3: Material properties: thermal characteristics of base fluid and nanoparticle materials (Ramzan *et al.* 2023; Hanif *et al.* 2024; Lund *et al.* 2024; Hyder *et al.* 2024)

Physical Properties	Water H_2O	Copper Cu	Alumina Al_2O_3	Titanium TiO_2
Thermal Expansion $\beta\,(K^{-1})$	2.1×10^{-4}	1.67×10^{-5}	8.5×10^{-6}	9.0×10^{-6}
Thermal Conductivity $k\,(Wm^{-1}K^{-1})$	0.613	400	40	8.9538
Density $\rho\,(kgm^{-3})$	997.1	8933	3970	4250
Specific Heat $C_p\,(Jkg^{-1}K^{-1})$	4179	385	765	686.2
Electrical Conductivity $\sigma\,(Sm^{-1})$	0.05	5.96×10^7	3.69×10^7	2.6×10^6

In practical scientific and engineering applications, the fundamental dimensionless quantities, namely the skin friction coefficient (C_f), and the Nusselt number (Nu), are formulated mathematically as presented in Mahmood *et al.* (2023).

$$C_f = \frac{\mu_{hnf}}{\rho_f u_e^2}\left(\frac{\partial u}{\partial y}\right)_{y=0}, \quad Nu = \frac{x q_w}{k_f(T_w - T_\infty)}. \tag{12}$$

here heat flux (q_w) fulfills the equation: $q_w = -\left(k_{hnf} + \frac{16\sigma^* T_\infty^3}{3k^*}\right)\left(\frac{\partial T}{\partial y}\right)_{y=0}$. After simplification, the locally defined Nusselt Number Nu_x is expressed as follows.

$$Nu_x = \sqrt{Re_x} Nu = -\left[\frac{k_{thnf}}{k_f}\right](1 + R_d)\,\theta'(0). \tag{13}$$

where $Re_x = \frac{u_w x}{\nu_f}$, and the local Skin Friction, denoted as C_{fx} , is expressed as follows:

$$C_{fx} = C_f \sqrt{Re_x} = \left[\frac{\mu_{thnf}}{\mu_f}\right] f''(0). \tag{14}$$

4. Numerical Approach: Keller Box Method

The nonlinear system of coupled ordinary differential equations, given by (9) and (10), together with the corresponding boundary conditions specified in (11), is solved numerically using the Keller box method. Originally proposed by Keller (1971) in 1971, this implicit finite difference scheme has been widely recognized for its accuracy and reliability in solving boundary layer problems involving nonlinear systems. The Keller box approach consists of several fundamental steps designed to approximate the solution, which can be outlined as follows:

(i) The original differential Eqs. (9) and (10), together with the boundary conditions (11), are first reformulated into a system of first order ordinary differential equations.
(ii) This system is then discretized using central finite difference approximations to derive a set of algebraic equations.
(iii) The resulting algebraic system is linearized through Newton's method, and the linearized equations are cast into a vectorized form suitable for numerical implementation.
(iv) The linear system is efficiently solved using the block tri diagonal elimination algorithm, which exploits the structural advantages of the discretized matrix system.

5. Results and Discussion

This study examines the fluid flow and heat transfer behavior of a THNF along an inclined surface that is either stretching or shrinking. Key influences such as thermal radiation, magnetohydrodynamic effects, suction or injection, shrinking/stretching, and the angle of inclination are incorporated into the analysis. The investigation focuses on velocity and temperature profiles, along with the evaluation of the skin friction coefficient and Nusselt number, under the following ranges of governing parameters: nanoparticle volume fractions $\phi_1 = \phi_2 = \phi_3 = 0.01$; thermal radiation parameter $0 \leq R_d \leq 2$; mixed convection parameter $0.5 \leq \lambda \leq 2.5$; inclination angle $\pi/6 \leq \gamma \leq \pi/3$; magnetic parameter $0 \leq M_g \leq 1$; suction or injection parameter $1.5 \leq s \leq 2.5$; stretching or shrinking parameter $-1.25 \leq \xi \leq 1.25$; and Prandtl number $Pr = 6.2$. These selected parameter values are consistent with those reported in earlier studies, enabling meaningful comparisons and contributing to a deeper understanding of THNF behavior. Relevant works in this context include Ben Ltaifa *et al.* (2021), Wahid *et al.* (2021), Alabdulhadi *et al.* (2021), Zainal *et al.* (2022), Ali *et al.* (2024a), and Asghar *et al.* (2022).

As explained in Table 4, the computed Nusselt number and skin friction coefficient from the current work were carefully checked with previously published data to confirm the accuracy of the numerical technique. The observed agreement confirms the reliability of the numerical approach used. Additionally, Table 5 highlights specific results for C_{fx} and Nu_x, offering a useful reference for researchers aiming to explore related phenomena in future investigations.

The effects of the suction/injection parameter and the inclination angle on the skin friction coefficient (C_{fx}) and the Nusselt number (Nu_x) are shown in Figure 2 and Figure 3, respectively. Analysis shows that rising the suction parameter shows a drop in C_{fx} with a rising tendency in Nu_x. The rising tendency in the Nusselt number is due to the suction effect that causes a more active fluid and surface interaction. Additional suction drags more fluid towards the wall boundary that improves convective flow around that location. The consequence is greater thermal transportation from the surface to the fluid and hence a rise in heat transfer rate and subsequently increasing the value of the Nusselt number (Iranian *et al.* 2023).

Table 4: Values of $f''(0)$ for a regular fluid, where $\mathrm{Pr} = 6.2$,with $\mathrm{Pr} = 6.2$, and M_g, R_d, ν, and λ set to 0

ξ	s	Roşca and Pop (2013)	Yasir *et al.* (2023)	present result
1	2	-2.4142	-2.41432	-2.4141347
	2.5	-2.8507	2.850701	-2.8506792
	3	-3.3027	-	-3.3026502
-1	2	1.0106	1.010631	1.0000006
	2.5	2	2	1.9998446
	3	2.618	2.618014	2.617873

Table 5: Values of local Nusselt number and skin friction, keeping $\phi_1 = \phi_2 = \phi_3 = 1\%$, and $Pr = 6.2$ for ternary hybrid nanofluid

γ	λ	s	M_g	R_d	ξ	C_{fx}	Nu_x
0	0	0	0	0	0	0	0.6817
$\pi/6$	1	2	1	3	-1	2.6515	2.3556
					1	-2.8489	3.511
$\pi/4$	2	2.5	2	2	-1	3.5317	4.453
					1	-3.5596	5.4786
$\pi/3$	3	3	3	1	-1	4.1907	8.4803
					1	-4.33	9.4716

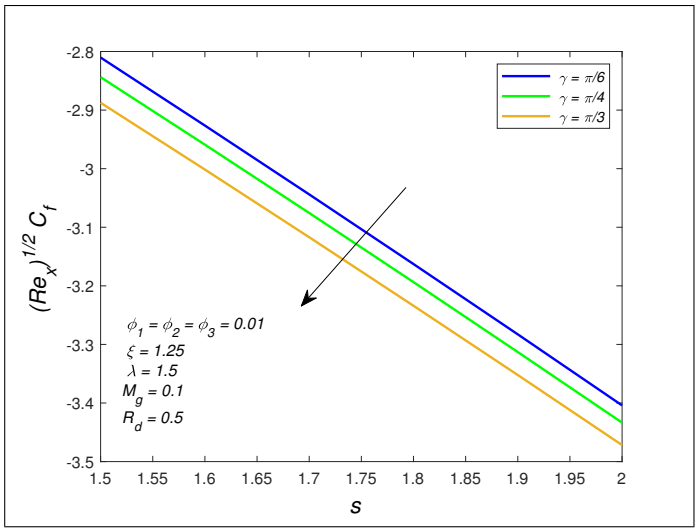

Figure 2: Effect of inclination angle (γ) and injection/suction parameter (s) on local skin friction (C_{fx})

Additionally, the effect of the inclination angle (γ) is explored. As the angle increases, both Nu_x and C_{fx} exhibit a downward trend. This behavior is associated with changes in buoyancy forces resulting from the modified orientation. A higher inclination introduces a buoyancy force component that acts against the primary flow, which weakens momentum and reduces the thickness of the thermal and velocity boundary layers. Hence, both the skin friction and heat transfer rate decline as the inclination angle becomes steeper. These observations hold practical relevance in heat transfer and fluid mechanics, providing engineers with valuable insight into optimizing thermal systems. By varying the inclination angle, they can fine tune both heat transfer efficiency and surface shear, leading to improved system effectiveness and reduced energy consumption. This is especially relevant for devices such as thermosyphons,

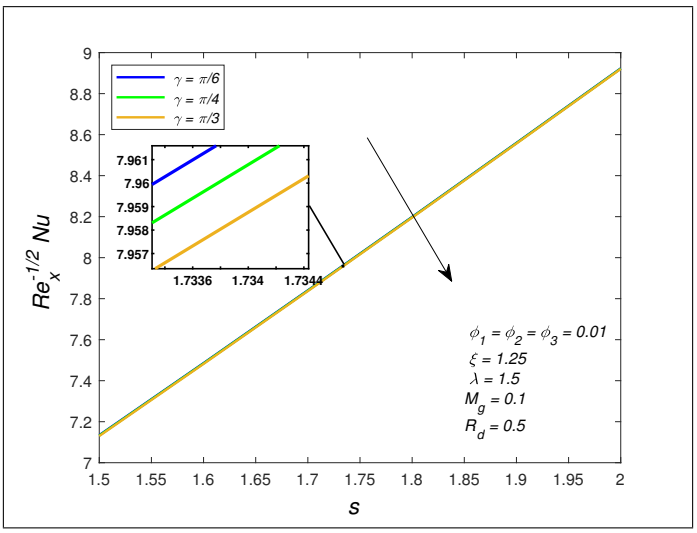

Figure 3: Effect of inclination angle (γ) and suction/injection parameter (s) on local Nusselt number (Nu_x)

whose functionality is derived through a blend of convection and conduction and phase change processes. The angle of inclination is a very important aspect of thermal behavior in them, influencing their ability to maintain efficient and stable heat transfer (Wu *et al.* 2019).

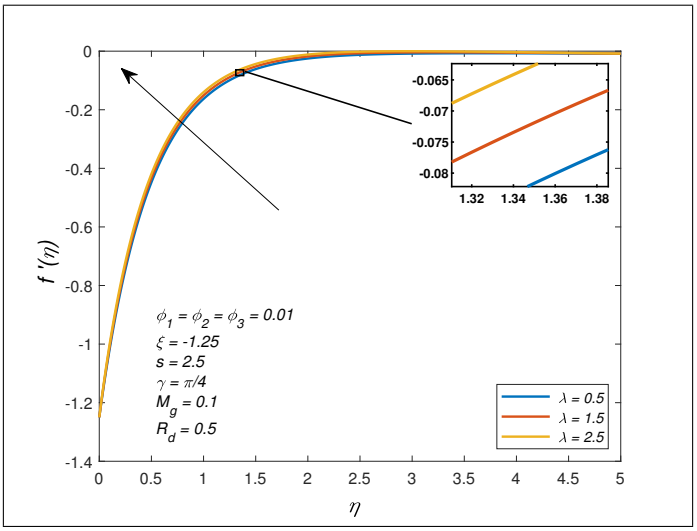

Figure 4: Effect of mixed convection parameter on velocity profiles

Figure 4 and Figure 5 show how the temperature profile $\theta(\eta)$ and velocity profile $f'(\eta)$ are affected by the mixed convection parameter (λ). Velocity is observed to increase with increasing λ, as indicated in Figure 4. This reveals that increased buoyancy forces, that is, higher λ, enhance fluid motion within the boundary layer.

Conversely, Figure 5 demonstrates a decline in temperature distribution as λ increases. This reduction can be attributed to the intensified buoyant force, which promotes fluid movement and facilitates greater thermal dissipation, thereby lowering the fluid temperature. Therefore, increasing the value of λ leads to a combination of enhanced velocity and reduced temperature, consistent with the findings reported in Venkata Ramudu *et al.* (2020).

As shown in Figure 6, the temperature profile $\theta(\eta)$ decreases with an increase in the stretch-

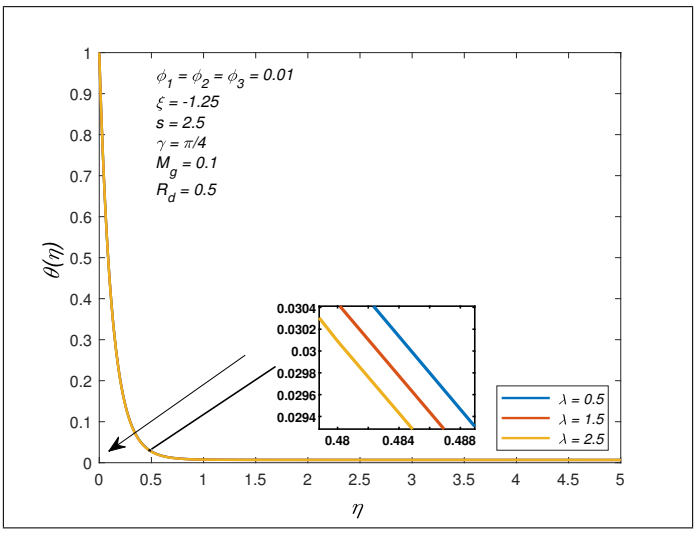

Figure 5: Effect of mixed convection parameter on temperature profiles

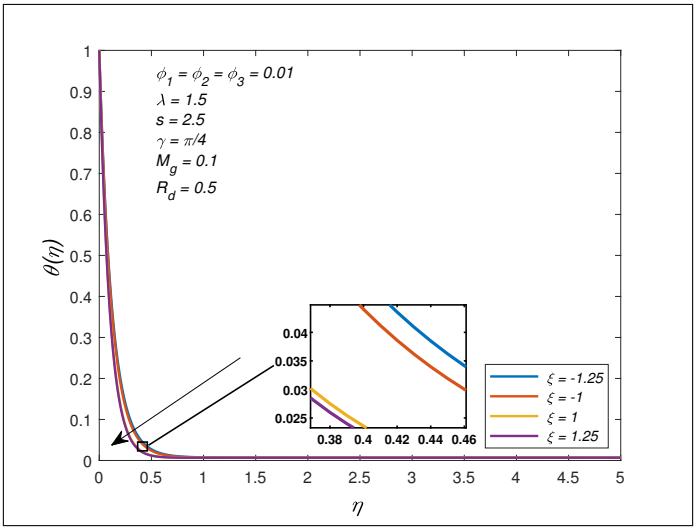

Figure 6: Effect of stretching/shrinking parameter on temperature profiles

ing or shrinking parameter ξ. In contrast, Figure 7 reveals that the velocity profile $f'(\eta)$ becomes more pronounced as ξ increases. This trend can be explained by two contributing factors. First, as the surface stretches more significantly, the flow near the wall becomes more organized and accelerated, which enhances the overall fluid velocity. This acceleration decreases the momentum boundary layer's thickness, resulting in higher velocity values. Second, a rise in ξ indicates that the free stream velocity is growing relative to the surface stretching speed. This relative increase contributes to further thinning of the boundary layer, reinforcing the growth in velocity profile. These observations are consistent with the analysis presented by Raju *et al.* (2016).

Figures 8 and 9 display the effect of the magnetic parameter M_g on the velocity and temperature distributions, respectively. As M_g increases, the velocity profile $f'(\eta)$ shows a rising trend. This can be linked to the reduction in momentum boundary layer thickness, which intensifies the velocity gradient near the surface and results in elevated fluid velocity. On the other hand, Figure 9 indicates that the temperature profile $\theta(\eta)$ decreases with higher values of M_g

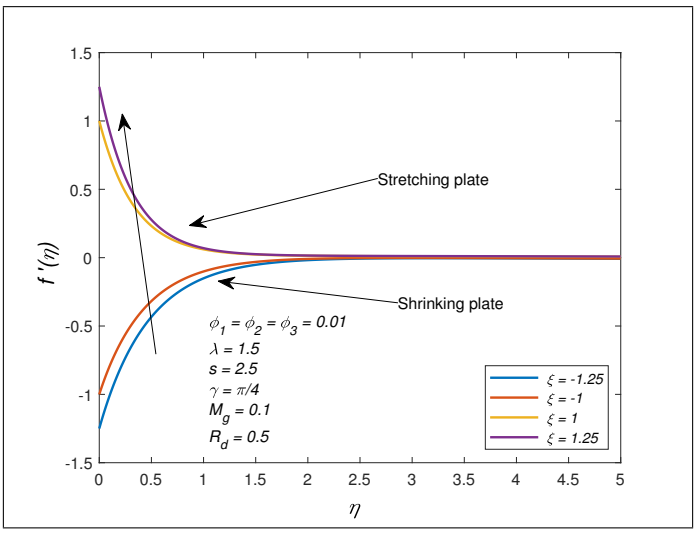

Figure 7: Effect of stretching/shrinking parameter on velocity profiles

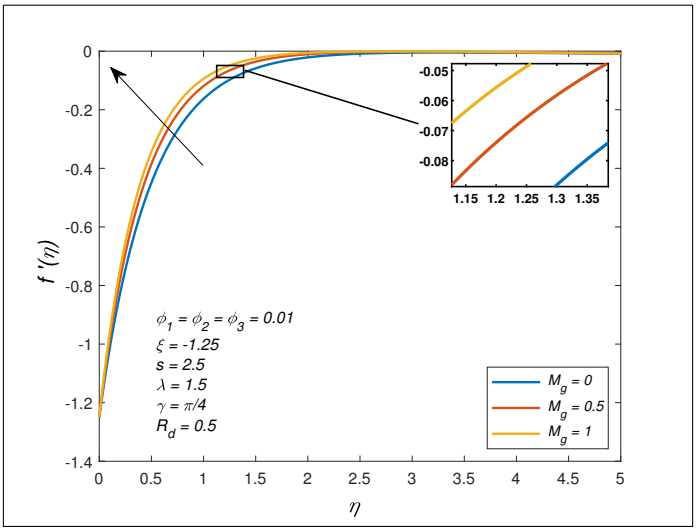

Figure 8: Effect of magnetic field (MHD) parameter on velocity profiles

within the boundary layer, aligning with observations reported in Sohut *et al.* (2023). However, this trend may vary depending on the surface condition. For instance, over a stretching surface, the thermal behavior might demonstrate an opposing pattern.

Figure 10 presents the variation in temperature profile corresponding to changes in the radiation parameter R_d. An increase in R_d leads to a noticeable rise in temperature. This behavior can be explained by the increased dominance of radiative heat transfer over conduction within the thermal boundary layer. When R_d becomes more significant, radiation contributes more effectively to heat release in the system, resulting in a net increase in fluid temperature (Ali *et al.* 2021a).

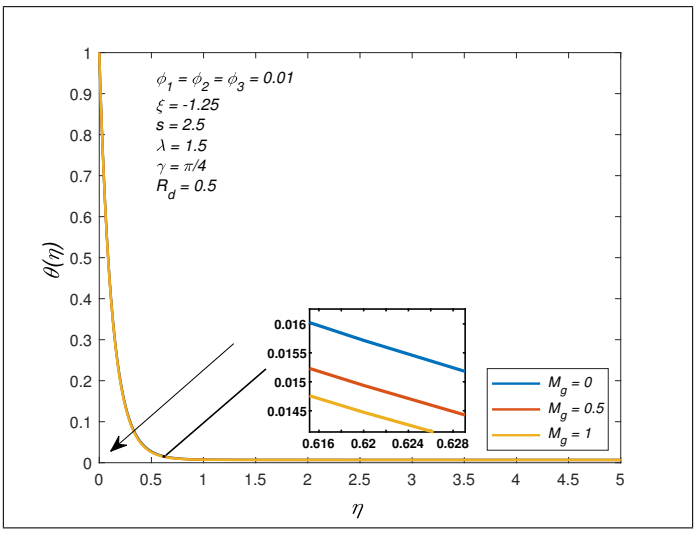

Figure 9: Effect of magnetic field (MHD) parameter on temperature profiles

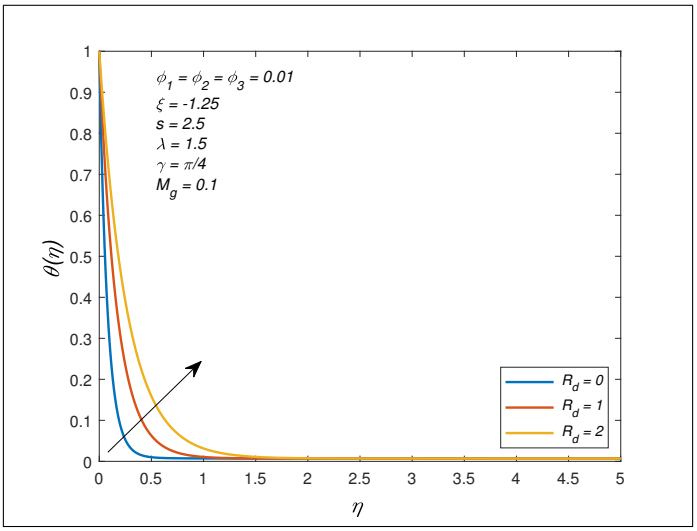

Figure 10: Effect of thermal radiation parameter on temperature profiles.

6. Conclusions

This study delves into the steady-state, two-dimensional mixed convection phenomena involving a ternary hybrid nanofluid (THNF) flowing past a vertical surface that experiences stretching or shrinking. The working fluid used is water, in which nanoparticles of titanium dioxide (TiO_2), aluminum oxide (Al_2O_3), and copper (Cu) are suspended. The governing equations, derived through appropriate similarity transformations, are tackled numerically via the Keller box scheme. The analysis examines the impacts of many dimensionless parameters including suction or injection rates, magnetic field intensity, and thermal radiation on the velocity field, temperature distribution, skin friction factor, and Nusselt number. The outcomes are depicted through graphical illustrations for enhanced clarity and ease of interpretation.

The principal conclusions reached from this investigation are summarized as follows:

- The skin friction coefficient (C_{fx}) decreases with an increase in both the suction param-

eter (s) and the inclination angle (γ).
- The Nusselt number (Nu_x) rises as the suction parameter (s) increases but declines with higher values of the inclination angle (γ).
- Velocity profiles ($f'(\eta)$) are enhanced with larger values of the mixed convection parameter (λ), while temperature profiles ($\theta(\eta)$) exhibit a downward trend as λ increases.
- A rise in the stretching or shrinking parameter (ξ) results in greater velocity profiles ($f'(\eta)$), whereas temperature profiles ($\theta(\eta)$) reduce with increasing ξ.
- As the magnetic parameter (M_g) increases, the velocity profiles ($f'(\eta)$) improve, while the temperature profiles ($\theta(\eta)$) show a decreasing trend.
- Temperature profiles ($\theta(\eta)$) increase steadily with higher values of the radiation parameter (R_d).

A key limitation of this study is the assumption that the concentration of nanoparticles remains constant throughout the fluid, which overlooks potential changes over time. Future research should examine how variations in nanoparticle concentration affect the thermal and flow properties of THNF. Additionally, incorporating the effects of the melting heat parameter could provide a more comprehensive understanding of heat transfer processes. Experimental investigations could further validate these findings, bridging the gap between theoretical models and practical applications.

Furthermore, this study highlights the critical impact of governing parameters, such as the inclined sheet angle and stretching/shrinking rates, on velocity and temperature profiles. These insights can guide the optimization of fluid flow and heat transfer systems in real-world applications, particularly in fields like solar thermal collectors, microchannel heat sinks, and energy storage systems, where enhanced thermal conductivity and controlled flow behavior are crucial (Saidur *et al.* 2011).

It is also recommended that future research explore the implications of the findings in contexts where non-uniform nanoparticle distribution and dynamic boundary conditions are prevalent. Addressing these aspects could improve the accuracy and applicability of THNF models. Limitations such as potential oversimplification of assumptions should be carefully addressed in subsequent studies, ensuring a closer alignment between theoretical predictions and experimental outcomes.

Acknowledgment

This research was funded by Universiti Teknologi Malaysia (UTM) and UTM Fundamental Research Vote No: Q.J130000.3854.23H57

References

Adnan, Abbas W., Said N.M., Mishra N.K., Mahmood Z. & Bilal M. 2024. Significance of coupled effects of resistive heating and perpendicular magnetic field on heat transfer process of mixed convective flow of ternary nanofluid. *Journal of Thermal Analysis and Calorimetry* **149**(2): 879–892.

Alabdulhadi S., Waini I., Ahmed S.E. & Ishak A. 2021. Hybrid nanofluid flow and heat transfer past an inclined surface. *Mathematics* **9**(24): 3176.

Algehyne E.A., Alrihieli H.F., Bilal M., Saeed A. & Weera W. 2022. Numerical approach toward ternary hybrid nanofluid flow using variable diffusion and non-Fourier's concept. *ACS Omega* **7**(33): 29380–29390.

Ali A., Afzaal M.F., Tariq F. & Hussain S. 2024a. Cattaneo-Christov heat flux and thermal radiation in MHD nanofluid flow over a bi-directional stretching/shrinking surface. *Journal of Nonlinear Mathematical Physics* **31**(1): 7.

Ali A., Kanwal T., Awais M., Shah Z., Kumam P. & Thounthong P. 2021a. Impact of thermal radiation and non-uniform heat flux on MHD hybrid nanofluid along a stretching cylinder. *Scientific Reports* **11**(1): 20262.

Ali B., Khan S.A., Hussein A.K., Thumma T. & Hussain S. 2022. Hybrid nanofluids: Significance of gravity modulation, heat source/sink, and magnetohydrodynamic on dynamics of micropolar fluid over an inclined surface via finite element simulation. *Applied Mathematics and Computation* **419**: 126878.

Ali B., Shafiq A., Siddique I., Al-Mdallal Q. & Jarad F. 2021b. Significance of suction/injection, gravity modulation, thermal radiation, and magnetohydrodynamic on dynamics of micropolar fluid subject to an inclined sheet via finite element approach. *Case Studies in Thermal Engineering* **28**: 101537.

Ali B., Siddique I., Saman I., Hussein A.K., Ghazwani H.A. & Ma B. 2024b. Significance of dust particles volume fraction to optimization of entropy in magnetohydrodynamic mixed convection flow via inclined surface. *Journal of Molecular Liquids* **394**: 123706.

Alqarni M.M., Memon A.A., Memon M.A., Mahmoud E.E. & Fenta A. 2023. Numerical investigation of heat transfer and fluid flow characteristics of ternary nanofluids through convergent and divergent channels. *Nanoscale Advances* **5**(24): 6897–6912.

Anuar N.S., Bachok N. & Pop I. 2021. Influence of buoyancy force on Ag-MgO/water hybrid nanofluid flow in an inclined permeable stretching/shrinking sheet. *International Communications in Heat and Mass Transfer* **123**: 105236.

Asghar A., Lund L.A., Shah Z., Vrinceanu N., Deebani W. & Shutaywi M. 2022. Effect of thermal radiation on three-dimensional magnetized rotating flow of a hybrid nanofluid. *Nanomaterials* **12**(9): 1566.

Ben Ltaifa K., D'Orazio A. & Dhahri H. 2021. Numerical analysis of mixed convection heat transfer and laminar flow in a rectangular inclined micro-channel totally filled with Water/Al2O3 nano fluid. *Journal of Thermal Analysis and Calorimetry* **144**: 2465–2482.

Chen H., He P., Shen M. & Ma Y. 2023. Thermal analysis and entropy generation of Darcy-Forchheimer ternary nanofluid flow: Acomparative study. *Case Studies in Thermal Engineering* **43**: 102795.

Das S., Ali A., Jana R.N. & Makinde O.D. 2022. EDL impact on mixed magneto-convection in a vertical channel using ternary hybrid nanofluid. *Chemical Engineering Journal Advances* **12**: 100412.

Dawar A., Islam S., Alshehri A., Bonyah E. & Shah Z. 2022. Heat transfer analysis of the MHD stagnation point flow of a non-newtonian tangent hyperbolic hybrid nanofluid past a non-isothermal flat plate with thermal radiation effect. *Journal of Nanomaterials* **2022**: 4903486.

Eid M.R., Jamshed W., Goud B.S., Ibrahim R.W., El Din S.M., Abd-Elmonem A. & Abdalla N.S.E. 2023. Mathematical analysis for energy transfer of micropolar magnetic viscous nanofluid flow on permeable inclined surface and Dufour impact. *Case Studies in Thermal Engineering* **49**: 103296.

Farooq U., Bibi A., Nawaz Abbasi J., Jan A. & Hussain M. 2024. Nonsimilar mixed convection analysis of ternary hybrid nanofluid flow near stagnation point over vertical Riga plate. *Multidiscipline Modeling in Materials and Structures* **20**(2): 261–278.

Hanif H., Khan A., Rijal Illias M. & Shafie S. 2024. Significance of Cu-Fe3O4 on fractional Maxwell fluid flow over a cone with Newtonian heating. *Journal of Taibah University for Science* **18**(1): 2285491.

Hanif H., Shafie S. & Jagun Z.T. 2023. Maximizing heat transfer and minimizing entropy generation in concentric cylinders with CuO-MgO-TiO2 nanoparticles. *Chinese Journal of Physics* **89**: 493–503.

Hyder A., Lim Y.J., Khan I. & Shafie S. 2023. Unveiling the performance of cu–water nanofluid flow with melting heat transfer, MHD, and thermal radiation over a stretching/shrinking sheet. *ACS Omega* **8**(32): 29424–29436.

Hyder A., Lim Y.J., Khan I. & Shafie S. 2024. Investigating heat transfer characteristics in nanofluid and hybrid nanofluid across melting stretching/shrinking boundaries. *BioNanoScience* **14**(2): 1181–1195.

Iranian D., Sudarmozhi K., Khan I. & Mohamed A. 2023. Significance of heat generation and impact of suction/injection on Maxwell fluid over a horizontal plate by the influence of radiation. *International Journal of Thermofluids* **20**: 100396.

Jeelani M.B. & Abbas A. 2023. Thermal efficiency of spherical nanoparticles Al2O3-Cu dispersion in ethylene glycol via the MHD non-Newtonian Maxwell fluid model past the stretching inclined sheet with suction effects in a porous space. *Processes* **11**(10): 2842.

Kadhim Hussein A., Pakdee W., Bechir Ben Hamida M., Ali B., Lafta Rashid F., Biswal U. & S Alhassan M. 2024. MHD mixed convection flow of alumina-water nanofluid into a lid-driven cavity with different patterns of wavy sidewalls. *Journal of Computational Applied Mechanics* **55**(1): 92–112.

Keller H.B. 1971. A new difference scheme for parabolic problems. In Bramble J. (ed.). *Numerical Solution of Partial Differential Equations–II*: 327-350. New York: Academic Press.

Lund L.A., Lashin M.M.A., Yashkun U., Guedri K., Khan S.U., Khan M.I., Bafakeeh O.T. & Kumam P. 2022.

Thermal stable properties of solid hybrid nanoparticles for mixed convection flow with slip features. *Scientific Reports* **12**(1): 16447.

Lund L.A., Omar Z., Khan U., Khan I., Baleanu D. & Nisar K.S. 2020. Stability analysis and dual solutions of micropolar nanofluid over the inclined stretching/shrinking surface with convective boundary condition. *Symmetry* **12**(1): 74.

Lund L.A., Yashkun U. & Shah N.A. 2024. Multiple solutions of unsteady Darcy–Forchheimer porous medium flow of Cu–Al2O3/water based hybrid nanofluid with Joule heating and viscous dissipation effect. *Journal of Thermal Analysis and Calorimetry* **149**(5): 2303–2315.

Mahmood Z., Eldin S.M., Rafique K. & Khan U. 2023. Numerical analysis of MHD tri-hybrid nanofluid over a nonlinear stretching/shrinking sheet with heat generation/absorption and slip conditions. *Alexandria Engineering Journal* **76**: 799–819.

Mishra A., Rawat S.K., Yaseen M. & Pant M. 2023. Development of machine learning algorithm for assessment of heat transfer of ternary hybrid nanofluid flow towards three different geometries: Case of artificial neural network. *Heliyon* **9**(11): e21453.

Nath R.S. & Deka R.K. 2024. A numerical study on the MHD ternary hybrid nanofluid (Cu-Al2O3-TiO2/H2O) in presence of thermal stratification and radiation across a vertically stretching cylinder in a porous medium. *East European Journal of Physics* (1): 232–242.

Noreen S., Farooq U., Waqas H., Fatima N., Alqurashi M.S., Imran M., Akgül A. & Bariq A. 2023. Comparative study of ternary hybrid nanofluids with role of thermal radiation and Cattaneo-Christov heat flux between double rotating disks. *Scientific Reports* **13**(1): 7795.

Ouyang Y., Basir M.F.M., Naganthran K. & Pop I. 2024a. Dual solutions in Maxwell ternary nanofluid flow with viscous dissipation and velocity slip past a stretching/shrinking sheet. *Alexandria Engineering Journal* **105**: 437–448.

Ouyang Y., Basir M.F.M., Naganthran K. & Pop I. 2024b. Triple solutions for unsteady stagnation flow of tri-hybrid nanofluid with heat generation/absorption in a porous medium. *Case Studies in Thermal Engineering* **61**: 105027.

Ouyang Y., Md Basir M.F., Naganthran K. & Pop I. 2024c. Unsteady magnetohydrodynamic tri-hybrid nanofluid flow past a moving wedge with viscous dissipation and Joule heating. *Physics of Fluids* **36**(6): 062009.

Raju C.S.K., Sandeep N. & Babu M.J. 2016. Stagnation point flow towards horizontal and exponentially stretching/shrinking cylinders. *Journal of Advanced Physics* **5**(3): 207–213.

Ramzan M., Kumam P., Lone S.A., Seangwattana T., Saeed A. & Galal A.M. 2023. A theoretical analysis of the ternary hybrid nanofluid flows over a non-isothermal and non-isosolutal multiple geometries. *Heliyon* **9**(4): e14875.

Roşca A.V. & Pop I. 2013. Flow and heat transfer over a vertical permeable stretching/shrinking sheet with a second order slip. *International Journal of Heat and Mass Transfer* **60**: 355–364.

Saidur R., Leong K.Y. & Mohammed H.A. 2011. A review on applications and challenges of nanofluids. *Renewable and sustainable energy reviews* **15**(3): 1646–1668.

Sarfraz M. & Khan M. 2023. Heat transfer efficiency in planar and axisymmetric ternary hybrid nanofluid flows. *Case Studies in Thermal Engineering* **44**: 102857.

Sohut F.H., Khan U., Ishak A., Soid S.K. & Waini I. 2023. Mixed convection hybrid nanofluid flow induced by an inclined cylinder with Lorentz forces. *Micromachines* **14**(5): 982.

Takreem M. & Satya Narayana P.V. 2024. Impact of Cattaneo-Christov heat flux on mixed convection flow of a ternary hybrid (Cu-Al2O3-TiO2/H2O) nanofluid over an elongated sheet: A comparative analysis. *Indian Journal of Chemical Technology (IJCT)* **31**(1): 57–69.

Usman M., Areshi M., Khan N. & Eldin M.S. 2023. Revolutionizing heat transfer: exploring ternary hybrid nanofluid slip flow on an inclined rotating disk with thermal radiation and viscous dissipation effects. *Journal of Thermal Analysis and Calorimetry* **148**(17): 9131–9144.

Vanitha G.P., Mahabaleshwar U.S. & Shadloo M.S. 2022. An impact of Richardson number on mixed convective flow of nanoparticles with heat and mass transfer. *International Communications in Heat and Mass Transfer* **139**: 106441.

Venkata Ramudu A.C., Anantha Kumar K., Sugunamma V. & Sandeep N. 2020. Influence of suction/injection on MHD Casson fluid flow over a vertical stretching surface. *Journal of Thermal Analysis and Calorimetry* **139**: 3675–3682.

Wahid N.S., Arifin N.M., Khashi'ie N.S. & Pop I. 2023. Mixed convection MHD hybrid nanofluid over a shrinking permeable inclined plate with thermal radiation effect. *Alexandria Engineering Journal* **66**: 769–783.

Wahid N.S., Arifin N.M., Khashi'ie N.S. & Pop I. 2021. Hybrid nanofluid slip flow over an exponentially stretching/shrinking permeable sheet with heat generation. *Mathematics* **9**(1): 30.

Wu Y., Zhang Z., Li W. & Xu D. 2019. Effect of the inclination angle on the steady-state heat transfer performance of a thermosyphon. *Applied Sciences* **9**(16): 3324.

Yasir M., Khan M., Alqahtani A.S. & Malik M.Y. 2023. Heat generation/absorption effects in thermally radiative mixed convective flow of Zn- TiO2/H2O hybrid nanofluid. *Case Studies in Thermal Engineering* **45**: 103000.

Zainal N.A., Nazar R., Naganthran K. & Pop I. 2022. The impact of thermal radiation on Maxwell hybrid nanofluids in the stagnation region. *Nanomaterials* **12**(7): 1109.

Department of Mathematical Sciences
Faculty of Science
Universiti Teknologi Malaysia
81310 Johor Bahru
Johor, MALAYSIA
E-mail: arfanhyder@graduate.utm.my, jiann@utm.my, sharidan@utm.my*

Department of Mathematics and Social Sciences
Sukkur IBA University
Sukkur 65200, PAKISTAN
E-mail: arfan.hyder@suk.edu.pk

Department of Mathematics
College of Science Al-Zulfi
Majmaah University
Al-Majmaah 11952, SAUDI ARABIA
E-mail: i.said@mu.edu.sa

Received: 3 February 2025
Accepted: 9 July 2025

*Corresponding author